

# Resistivity dependent dielectric and magnetic properties of $\text{Pb}(\text{Fe}_{0.012}\text{Ti}_{0.988})\text{O}_3$ nanoparticles

K. C. Verma,<sup>1,a)</sup> R. K. Kotnala,<sup>2</sup> N. Thakur,<sup>1</sup> V. S. Rangra,<sup>1</sup> and N. S. Negi<sup>1</sup>

<sup>1</sup>Department of Physics, Himachal Pradesh University, Shimla 171005, India

<sup>2</sup>National Physical Laboratory, New Delhi 110012, India

(Received 21 March 2008; accepted 20 May 2008; published online 6 November 2008)

High resistivity in nanostructured  $\text{Pb}(\text{Fe}_{0.012}\text{Ti}_{0.988})\text{O}_3$  system prepared by using polyvinyl alcohol (PVA) in chemical route is observed. The PVA acts as a surfactant to limit the particle size. The Fe substitution for Ti controls the chemical stoichiometry and reduces the lattice distortion, i.e.,  $c/a$  ratio, and hence the transition temperature reduces with Fe content. The phase structure, morphology, particle size, dc resistivity, and dielectric and magnetic properties of  $\text{Pb}(\text{Fe}_{0.012}\text{Ti}_{0.988})\text{O}_3$  nanoparticles have been characterized by x-ray diffraction, transmission/scanning electron microscopy, source meter, LCR meter, and vibrating sample magnetometer. The results indicate that the nanosize particles have high resistivity, which improves the dielectric constant at high-frequency region and increases magnetization of the specimens. The observed variable-range-hopping conduction mechanism indicates that Fe doping leads to the occurrence of local defect states in the  $\text{PbTiO}_3$  lattice. The dispersionless dielectric properties with low loss are observed up to 15 MHz. The dielectric properties are improved than those obtained by the conventional process. The initial permeability values do not exhibit much variation up to ferromagnetic transition temperature after which it falls sharply. The large value of saturation magnetization is observed at room temperature. © 2008 American Institute of Physics. [DOI: 10.1063/1.2961328]

## I. INTRODUCTION

Multiferroic materials exhibit the properties of ferroelectricity, ferromagnetism, and ferroelasticity within a single phase. The current technological trend is to exclude the requirement of ferroelasticity in memory device applications. Recently multiferroic materials have become the focus of much interest due to their potential applications in spintronics, storage devices, sensors, transducers, and actuators.<sup>1-4</sup> The most fascinating applications of these materials are in new types of storage media using both magnetic and electric polarizations through their coupling. The coupling of magnetization and polarization could in principle allow data to be written electrically and read magnetically, thus overcome the difficulties associated with reading ferroelectric random access memory and requiring large magnetic field to write magnetic data storage. The single-phase materials in which ferroelectricity and ferromagnetism exist are rare and mostly possess rather weak ferromagnetism.<sup>5,6</sup> The important multiferroic oxides studied until now include  $\text{BiFeO}_3$ ,  $\text{SeCuO}_3$ ,  $\text{RMnO}_3$ ,  $\text{RMn}_2\text{O}_5$  (R=rare earth, Y, and Bi), etc.<sup>7-10</sup> Among them,  $\text{BiFeO}_3$  has been most extensively studied due to its simple structure, a high ferroelectric Curie temperature ( $T_c = 830^\circ\text{C}$ ) and a high Neel temperature ( $T_N = 370^\circ\text{C}$ ). The major problem with  $\text{BiFeO}_3$  is its low electrical resistivity which makes it difficult to obtain a well saturated ferroelectric hysteresis loop and a high dielectric loss and thus limits its practical applications.<sup>11,12</sup> To overcome the scarcity of

single-phase multiferroics, two approaches are suggested. One approach is to enhance the specific characteristics of  $\text{BiFeO}_3$  and other multiferroics by doping.<sup>13</sup> The other is the development of new multiferroic materials such as ferroelectric-ferromagnetic heterostructure.<sup>14</sup> On other hand, Pb-based compounds such as  $\text{PbTiO}_3$  has been thoroughly studied for ferroelectric memories and other applications besides their environment limitations. Thus the substitutions of Ti in  $\text{PbTiO}_3$  system by transition metal elements such as Fe, Ni, Co, etc., could be an approach to search for new multiferroic compounds. In recent years, a few studies have been carried out to investigate on multiferroic properties of Fe substituted  $\text{PbTiO}_3$  system. Palkar *et al.*<sup>15</sup> have first observed magnetoelectric properties in ferroelectric  $\text{PbTiO}_3$  by partially substituting Ti with Fe. Ren *et al.*<sup>16</sup> showed room temperature ferromagnetism in Fe doped  $\text{PbTiO}_3$  nanocrystals prepared by hydrothermal method using polyethylene glycol as surfactant. In our earlier work, we report enhance dielectric and ferromagnetic properties of Fe doped  $\text{PbTiO}_3$  nanoparticles prepared by using polyvinyl alcohol (PVA) as a surfactant.<sup>17</sup> The substitution of Fe at Ti site reduces lattice distortion. However,  $\text{PbTiO}_3$  exhibits a very large lattice distortion ( $c/a \sim 1.064$ ). It is believed that with nominal Fe substitution in  $\text{PbTiO}_3$  could still maintain its tetragonal distortion to some extent while making it to induce magnetism without disturbing its ferroelectric properties. Although a lot of work have been reported on synthesis of multiferroic  $\text{Pb}(\text{Fe}_{0.012}\text{Ti}_{0.988})\text{O}_3$  system, there is no report on the resistivity dependent dielectric and magnetic properties of the system.

Therefore an attempt has been made to synthesize a

<sup>a)</sup> Author to whom correspondences should be addressed. Tel.: +91 0177 2830950. FAX: +91 0177 2830775. Electronic mail: kuldeep0309@yahoo.co.in.

nanostructured  $\text{Pb}(\text{Fe}_{0.012}\text{Ti}_{0.988})\text{O}_3$  by chemical route using PVA as a surfactant to limit the particle size. We present here dielectric and magnetic properties of  $\text{Pb}(\text{Fe}_{0.012}\text{Ti}_{0.988})\text{O}_3$  system in details. The results are discussed within the framework of magnetoelectric system.

## II. EXPERIMENT

Lead acetate, tetra-*n*-butyl orthotitanate ( $\text{C}_{16}\text{H}_{36}\text{O}_4\text{Ti}$ ) and ferric chloride were used to prepare precursor solution of  $\text{Pb}(\text{Fe}_{0.012}\text{Ti}_{0.988})\text{O}_3$ . In the first step, ethyl alcohol and acetic acid solutions were mixed in the volume ratio of 75:25, respectively. In this solution, a calculated amount of tetra-*n*-butyl orthotitanate was added and the mixture (A) was stirred for 2 h. Another solution was prepared by taking proportional amount of lead acetate and distilled water. Additional 20 mol % excess of lead was also added to compensate the Pb loss during the processing and to assist the crystallization. The solution was then poured into the first solution and the resulting mixture (B) was stirred for 2 h. Finally, the solution of ferric chloride added to the mixture B was stirred for 1 h. The solution was clear and transparent at room temperature. In the second step, PVA solution was added to encapsulate the cationic species in divided groups. For preparing PVA solution, 0.25 g PVA was taken in a beaker containing 20  $\text{cm}^3$  of distilled water. The mixture was rigorously stirred and the temperature was slowly raised to 80 °C. The stirring and heating were continued until the PVA was completely dissolved in water. The solution obtained from first step was then poured into a separately prepared transparent PVA solution in 5:2 volume ratios, respectively, to form the final mixture. The final solution was a clear gel at room temperature. The gel was dried at 250 °C and heated at 700 °C for 2 h for crystallization.

The crystalline structure of the specimen was analyzed by x-ray diffraction (XRD) using X-Pert PRO system. The average value of grain size of the crystallites ( $D$ ) was calculated by using Debye–Scherer relation,<sup>18</sup>

$$D = \frac{0.9\lambda}{\beta \cos \theta}, \quad (1)$$

where  $\lambda$  is the wavelength and  $\theta$  is the angle of diffraction. The microstructural properties were investigated by using transmission/scanning electron microscopes (TEM/SEM) (Hitachi H-7500/JEOL JSM6100). The powder of  $\text{Pb}(\text{Fe}_{0.012}\text{Ti}_{0.988})\text{O}_3$  heated at 700 °C was pressed into pellet and torroid forms using a pressure of 5 bars for 10 min. The pellet and torroid were then sintered at higher temperature of ~1000 °C for 5 h. The dielectric properties and permeability of the specimen were measured in the range of room temperature to transition temperature by using a LCR meter (Agilent: 4285A) over frequency range of 0.075–16 MHz. The saturation magnetization ( $M_s$ ) loop of Fe doped  $\text{PbTiO}_3$  nanoparticles was measured at room temperature using a vibrating sample magnetometer (VSM-735). The variation of dc resistivity with temperature was measured by using a Keithley 2611 source meter.

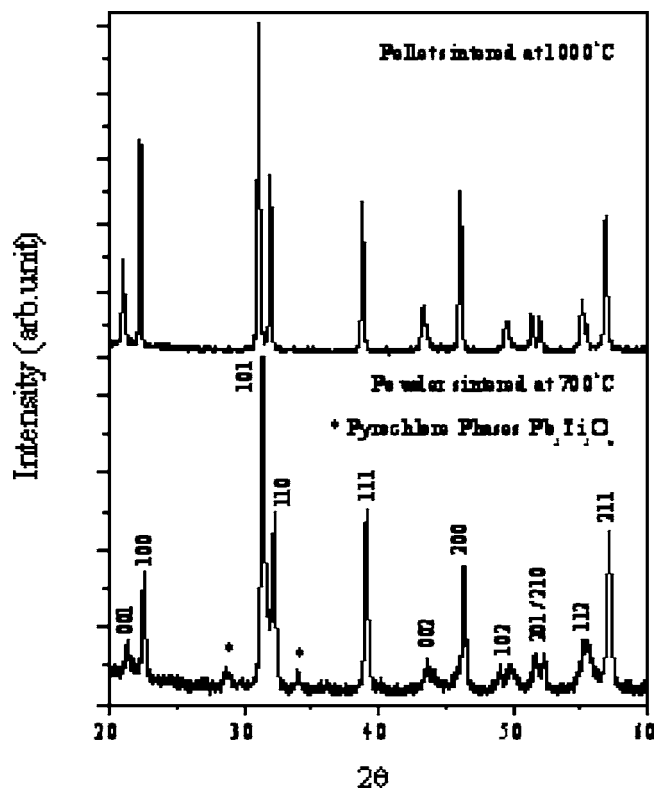


FIG. 1. XRD of  $\text{Pb}(\text{Fe}_{0.012}\text{Ti}_{0.988})\text{O}_3$  nanoparticles.

## III. RESULTS AND DISCUSSION

Figure 1 shows the XRD spectra of the powder and pellet of nanostructured  $\text{Pb}(\text{Fe}_{0.012}\text{Ti}_{0.988})\text{O}_3$  sintered at 700 and 1000 °C, respectively. The XRD patterns which indicate a tetragonal perovskite structure ( $c/a=1.058$ ) for present system and all reflections (001), (100), (101), (110), (111), (002), (200), and (102) are observed at diffraction angles  $2\theta=21.43^\circ$ ,  $22.77^\circ$ ,  $31.45^\circ$ ,  $32.41^\circ$ ,  $39.18^\circ$ ,  $43.62^\circ$ ,  $46.51^\circ$  and  $50.17^\circ$ , respectively, and are well matched with the ASTM card. Extra peaks observed in powder sample heated at 700 °C correspond to a minor pyrochlore  $\text{Pb}_2\text{Ti}_2\text{O}_6$  impurity phase. The pellet sample has been sintered at higher temperature of ~1000 °C for 5 h in air. The XRD pattern of pellet sintered at higher temperatures appears perovskite without any pyrochlore phase. The pyrochlore phase at 700 °C is due to a low sintering temperature, which diminishes on increasing the temperature to 1000 °C. The similar impurity phase was also observed in  $\text{Pb}(\text{Fe Ti})\text{O}_3$  system by Palkar *et al.*<sup>15</sup> The particle size was calculated from XRD peak broadening using Scherer's formula as in Eq. (1). The average particle's sizes in the powder (sintered at 700 °C) and pellet (sintered at 1000 °C) are ~24 and ~35 nm, respectively. It infers that the particle size still lies in the range of nanometers even at a high sintering temperature of 1000 °C. The TEM and SEM of the powder specimen heated at 700 °C are shown in Figs. 2(a) and 2(b), respectively. The values of the particle size as obtained from TEM/SEM images are in good agreement with the one, calculated from XRD patterns. The observed particle size is much smaller than that reported by Ren *et al.*<sup>16</sup> The significant reduction in particle size may be attributed to PVA as surfac-

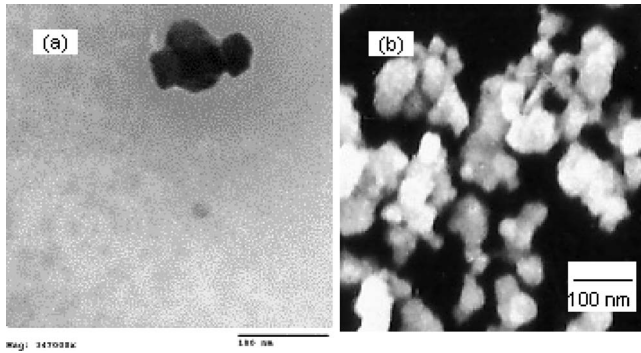


FIG. 2. (a) TEM for  $\text{Pb}(\text{Fe}_{0.012}\text{Ti}_{0.988})\text{O}_3$  powder sintered at  $700^\circ\text{C}$ . (b) SEM for  $\text{Pb}(\text{Fe}_{0.012}\text{Ti}_{0.988})\text{O}_3$  powder sintered at  $700^\circ\text{C}$ .

tant in present processing technique. Mu *et al.*<sup>19</sup> reported that PVA when used as a surfactant is more efficient in surface modification and in reduction of particle size than polyethylene glycol as surfactant by Ren *et al.*<sup>16</sup>

Figure 3 shows the variation of dc resistivity of specimen over temperature range of 298–423 K. The dc resistivity is measured in the range of  $10^{10}$   $\Omega$  cm. The high resistivity is consistent with that reported in literature.<sup>20</sup> Materials with smaller grain size contain relatively larger volume fraction in between the grains, which act as a barrier for current conduction. This results in an increase in the resistivity. The high resistivity which, reduces the eddy current losses, makes the multiferroic material more suitable for high-frequency applications.

The results of the temperature dependence of the resistivity cannot be discussed by general mechanism  $\rho = \rho_0 \exp(E_c/K_B T)$ , which is commonly employed to analyzed the conduction band, because activation energy  $< E_c$  of bulk  $\text{PbTiO}_3$  is observed in the present system. However, a satisfactory result is obtained by fitting the experimental data in equation described by Mott and Davis<sup>21</sup> for a variable-range-hopping (VRH) conduction mechanism, defined as

$$\rho = \rho_0 \exp\left(\frac{B}{T^{1/4}}\right), \quad (2)$$

where  $B=4E/(K_B T^{3/4})$  and  $E$  is the activation energy for VRH. The plot  $\log_{10}(\rho_{dc})$  versus  $1/T^{1/4}$  thus obtained shows a straight lines over a considerable temperature range [Fig. 3 (inset)]. In the VRH model, it is assumed that the charge carriers move away along a path determined by the optimal pair hopping rate from one localized state to another in the disorder system. This type of conduction is generally observed in some amorphous materials due to states in the gap because of divacancies and dangling bonds. In other words, it arises from lattice disorder. In  $\text{Pb}(\text{Fe}_{0.012}\text{Ti}_{0.988})\text{O}_3$  system number of factors have to be considered: first, creation of Pb vacancies due to PbO loss; second, oxygen vacancies are easily formed due to oxygen loss at high sintering temperature in order to balance the charge inquilines arise from Pb vacancies; third, in Ti based materials Ti can easily change its valence. This result in electron jump between  $\text{Ti}^{4+} \leftrightarrow \text{Ti}^{3+}$  and / or  $\text{Fe}^{4+} \leftrightarrow \text{Fe}^{3+}$  might be possible. The activation energy as calculated by applying VRH mechanism is  $E = 0.51$  meV in the lower temperature region of 300 K, which increases to 0.67 meV at higher temperature region of 423 K. The value of activation energy is less than  $E_c$ , which suggest that conduction in present system can be described by VRH mechanism. The disorder system of  $\text{Pb}(\text{Fe Ti})\text{O}_3$  with random distribution of  $V_{\text{pb}}$  and Fe ions having long-range movement of the weakly bonded electrons give the dc conduction, which can be understood by the VRH mechanism. The similar behavior is also observed in  $\text{SrFeO}_3$  semiconducting system by Liu *et al.*<sup>22</sup> The observed VRH phenomenon implies, therefore, that the  $\text{Pb}(\text{Fe}_{0.012}\text{Ti}_{0.988})\text{O}_3$  material is highly disordered, with the disorder coming probably from the existence of Pb vacancies, oxygen vacancies, and the random distribution of the Ti and Fe ions.

The frequency dependence dielectric constant ( $\epsilon$ ) and dielectric loss ( $\tan \delta$ ) of  $\text{Pb}(\text{Fe}_{0.012}\text{Ti}_{0.988})\text{O}_3$  nanoparticles have been measured at room temperature in the frequency range of 0.075–16 MHz and is presented in Fig. 4(a). No dispersion in the dielectric constant value can be seen over the frequency range from 0.075 to 15 MHz. The measured dielectric constant value is 47. This dielectric response may be attributed to the absence of space charge polarization in the highly resistive specimens. At frequency  $> 15$  MHz, the abrupt change in dielectric constant is due to dielectric relaxation. The short-range hopping of weakly bonded defects through  $\text{Ti}^{4+} \leftrightarrow \text{Ti}^{3+}$  and  $\text{Fe}^{4+} \leftrightarrow \text{Fe}^{3+}$  leads to a net dipole moment, which originates the permittivity relaxation peak contributed by defect states controlled ac conduction. In our measurements, we have observed dispersionless dielectric properties up to 15 MHz, which is an improvement over the conventionally prepared specimens.<sup>23</sup> The loss factor is quite low (0.003) at frequency  $< 15$  MHz. The upward rise in  $\tan \delta$  at frequency  $> 15$  MHz is due to dielectric relaxation discussed earlier.

The temperature dependence of dielectric constant and dielectric loss at different frequencies are shown in Figs. 4(b) and 4(c). It is observed that the dielectric constant increases with increasing temperature for all frequencies. Dielectric

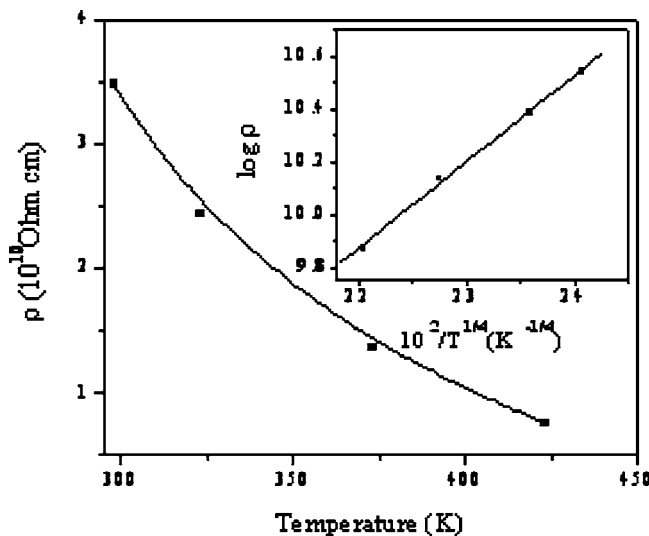


FIG. 3. Variation of dc resistivity with temperature. Plot of  $\log \rho$  vs  $10^2/T^{1/4}$  ( $\text{K}^{-1/4}$ ) (inset).

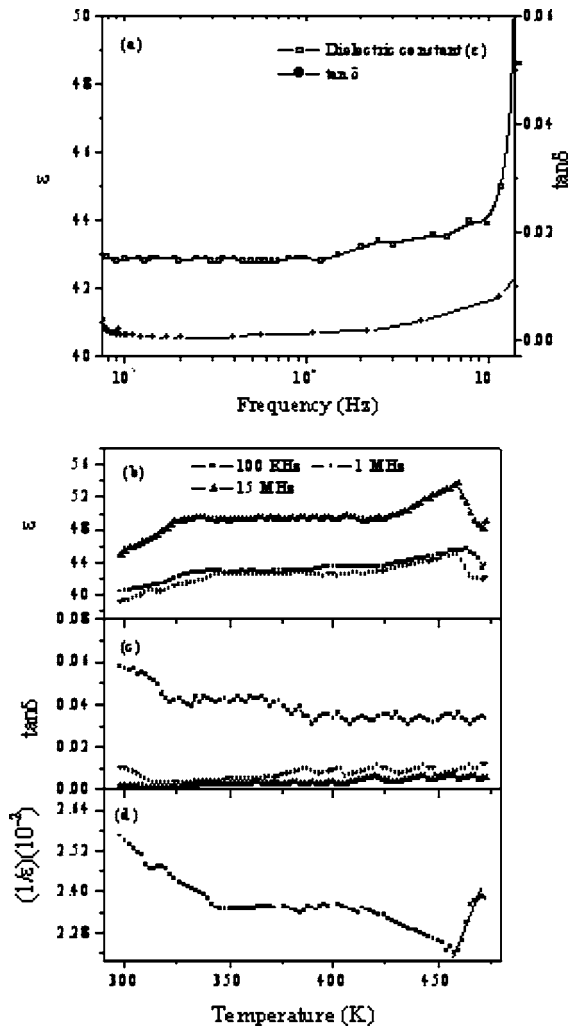


FIG. 4. (a) Variation of dielectric constant ( $\epsilon$ ) and dielectric loss ( $\tan \delta$ ) as the function of frequency at room temperature. (b) Variation of dielectric constant ( $\epsilon$ ) as the function of temperature. (c) Variation of dielectric loss ( $\tan \delta$ ) as the function of temperature. (d) Inverse permittivity with temperature (fitted with Curie–Weiss law) at frequency of 1 MHz.

measurements show peaks around 460 K, which could be due to ferroelectric phase transition temperature. It is confirmed that the ferroelectric phase transition temperature is quite low compared to the pure  $\text{PbTiO}_3$ , which has Curie temperature of 763 K.<sup>24</sup> This is due to Fe substitutions in  $\text{PbTiO}_3$ , which can minimize superposition of electric domains and, hence, such dielectric behavior is due to reduced domains.<sup>20</sup>

For a typical ferroelectric, the Curie–Weiss law,

$$\frac{1}{\epsilon} = \frac{(T - T_0)}{C}, \tag{3}$$

where  $T_0$  is the Curie–Weiss temperature and  $C$  is the curie constant. A  $T_0$  of 722 K and a  $C$  of  $4.1 \times 10^5 \text{ }^\circ\text{C}$  have been obtained for pure  $\text{PbTiO}_3$  crystal.<sup>25</sup> For the  $\text{Pb}(\text{Fe}_{0.012}\text{Ti}_{0.988})\text{O}_3$  nanoparticles, the real part of the dielectric permittivity ( $\epsilon$ ) was fitted to the Curie–Weiss law [Fig. 4(d)] at 1 MHz. The fitting parameters are  $T_0=454 \text{ K}$ ,  $C = 4.9 \times 10^5 \text{ }^\circ\text{C}$ , and  $\Delta T_m = T_{\text{dev}} - T_{\text{em}} = 6 \text{ K}$ . Hence, the deviation from Curie–Weiss law suggests the absence of space

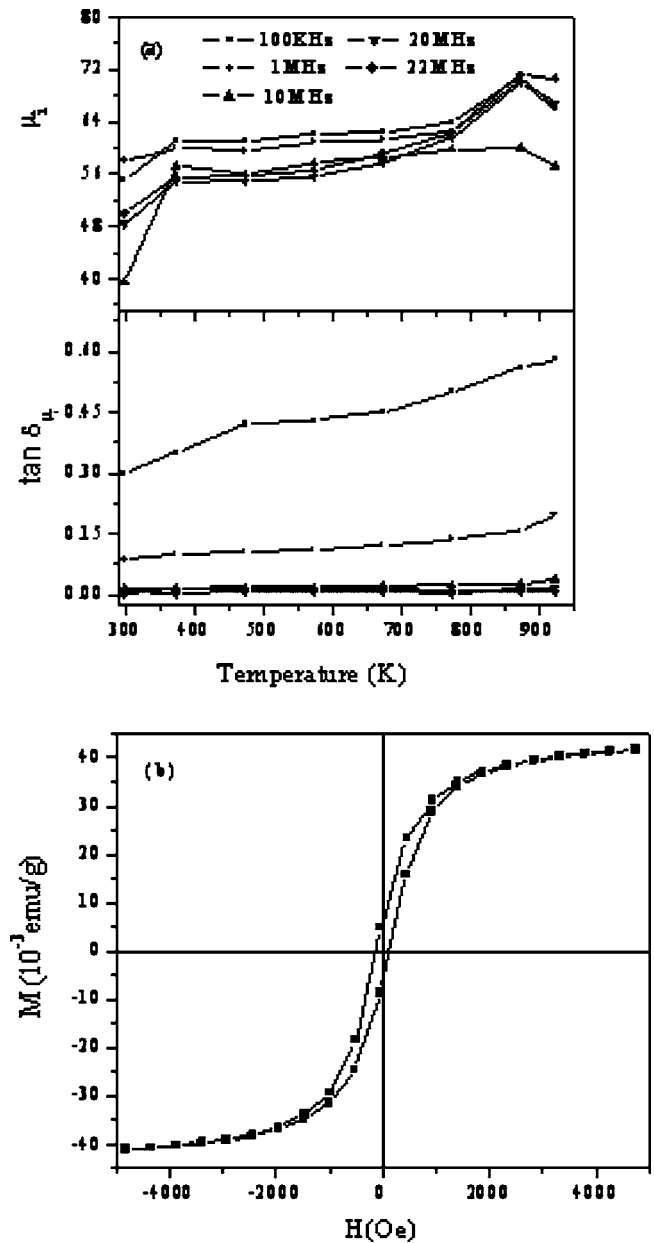


FIG. 5. (a) Variation of initial permeability ( $\mu_i$ ) and magnetite loss factor ( $\tan \delta\mu_i$ ) with temperature. (b) Room temperature magnetization-field ( $M$ - $H$ ) curve for  $\text{Pb}(\text{Fe}_{0.012}\text{Ti}_{0.988})\text{O}_3$  nanoparticles sintered at  $700 \text{ }^\circ\text{C}$ .

charge polarization in the specimen. Similar behavior is also found in dielectric loss.

The variation in initial permeability ( $\mu_i$ ) and its loss ( $\tan \delta\mu_i$ ) with rise in temperature at different frequencies is shown in Fig. 5(a). The initial permeability is found to increase with an increase in temperature at all the frequencies, as is expected. But at temperature about 470 K, the saturation in permeability curve was observed. Hence dielectric measurements as a function of temperature were carried out in Fig. 4(b), which reveal a broad peak around 460 K. In magnetoelectrically ordered systems, the magnetic anomaly near dielectric transition is predicted by Landau–Devonshire theory of phase transition.<sup>26</sup> At the temperature of 873 K, called the ferromagnetic transition temperature ( $T_c$ ), it attains a maximum value, after which initial permeability falls sharply. Such behavior is usual in most of the magnetic ma-



materials. Initial permeability increases with the rising temperature to a peak value just below the transition temperature and then decreases to  $\mu_0$  above transition temperature.<sup>27</sup> Bhide *et al.*<sup>28</sup> observed that the existence of  $\text{Fe}^{4+}$  and  $\text{Fe}^{3+}$  ions which are in the equilibrium charge states and the impurity charge carriers moves only within the local environment having quadrupole splitting, which is found to persist beyond  $T_C$ . This results a small reduction in ferromagnetic transition temperature. The loss factor is usually expressed in terms of the eddy current loss that gives rise to a loss tangent proportional to frequency. The resistivity of the material is a more useful parameter than the eddy current, thus, these small values of loss are expected due to the high resistivity of the nanomultiferroic.

The hysteresis loop of the  $\text{Pb}(\text{Fe}_{0.012}\text{Ti}_{0.988})\text{O}_3$  nanoparticles measured at room temperature is illustrated in Fig. 5(b). It shows large saturation magnetization value  $M_s = 41.6 \times 10^{-3}$  emu/g ( $0.52 \mu_B/\text{Fe}$ ) and low coercivity ( $H_c \sim 125.3$  Oe). The observed value of saturation magnetization is significantly higher than value  $\approx 0.8 \times 10^{-3}$  emu/g ( $0.01 \mu_B/\text{Fe}$ ) reported by Ren *et al.* for their hydrothermally prepared Fe doped nanocrystals of  $\sim 100$  nm. Nanosized magnetoelectric material causes superparamagnetic relaxation contribute to least the hysteresis than ferromagnetic.<sup>29</sup> The enhancement in ferromagnetic properties is due to the smaller particle size in our specimen.

#### IV. CONCLUSION

Nanostructured  $\text{Pb}(\text{Fe}_{0.012}\text{Ti}_{0.988})\text{O}_3$  was synthesized by using PVA as a surfactant. The average particle size as measured by XRD and TEM/SEM is  $\sim 24$  nm. The dc resistivity is found to be  $\sim 3.47 \times 10^{10}$   $\Omega$  cm and enhancements in dielectric and magnetic properties with low loss are observed. The improvement in dielectric and magnetic properties of nanostructured  $\text{Pb}(\text{Fe}_{0.012}\text{Ti}_{0.988})\text{O}_3$  may be attributed to the high value of resistivity. The VRH conduction mechanism suggests that the  $\text{Pb}(\text{Fe}_{0.012}\text{Ti}_{0.988})\text{O}_3$  system consists of

some localized states due to Pb vacancies. The improvement in room temperature ferromagnetism is also observed.

- <sup>1</sup>M. Li, M. Ning, Y. Ma, Q. Wu, and C. K. Ong, *J. Phys. D* **40**, 1603 (2007).
- <sup>2</sup>M. Fiebig, T. Lottermoser, D. Frohlich, A. V. Golesev, and R. V. Pisarev, *Nature (London)* **419**, 818 (2002).
- <sup>3</sup>N. Hur, S. Park, P. A. Sharma, J. S. Ahn, S. Guha, and S. W. Cheong, *Nature (London)* **429**, 392 (2004).
- <sup>4</sup>S. Dong, J. Zhai, J. F. Li, D. Viehland, and M. I. Bichurim, *Appl. Phys. Lett.* **89**, 243512 (2006).
- <sup>5</sup>N. A. Spaldin and M. Fiebig, *Science* **309**, 391 (2005).
- <sup>6</sup>N. A. Hill, *J. Phys. Chem. B* **104**, 6694 (2000).
- <sup>7</sup>J. Wang, J. B. Neaton, and R. Ramesh, *Science* **299**, 1719 (2003).
- <sup>8</sup>G. Lawes, A. P. Ramirez, C. M. Verma, and M. A. Subramanian, *Phys. Rev. Lett.* **91**, 257208 (2003).
- <sup>9</sup>T. Kimura, S. Kawamoto, I. Yamada, M. Azuma, M. Takano, and Y. Tokura, *Phys. Rev. B* **67**, 180401 (2003).
- <sup>10</sup>N. Hur, S. Park, P. A. Sharma, S. Guha, and S. W. Cheong, *Phys. Rev. Lett.* **93**, 107207 (2004).
- <sup>11</sup>A. K. Pradhan, K. Zhang, D. Hunter, J. B. Dadson, G. B. Loiutts, P. Bhattacharya, R. Katiyar, J. Zhang, D. J. Sellmyer, U. N. Roy, Y. Cui, and A. Burger, *J. Appl. Phys.* **97**, 093903 (2005).
- <sup>12</sup>V. R. Palkar, J. John, and R. Pinto, *Appl. Phys. Lett.* **80**, 1628 (2002).
- <sup>13</sup>Y. K. Jun, W. T. Moon, C. M. Chang, H. S. Kim, H. S. Ryu, J. W. Kim, K. H. Kim, and S. H. Hong, *Solid State Commun.* **135**, 133 (2005).
- <sup>14</sup>S. Dong, J. F. Li, and D. Viehland, *Appl. Phys. Lett.* **83**, 2265 (2003).
- <sup>15</sup>V. R. Palkar and S. K. Malik, *Solid State Commun.* **134**, 783 (2005).
- <sup>16</sup>Z. Ren, G. Xu, X. Wei, Y. Liu, X. Hou, P. Du, W. Weng, G. Shen, and G. Han, *Appl. Phys. Lett.* **91**, 063106 (2007).
- <sup>17</sup>K. C. Verma, R. K. Kotnala, and N. S. Negi, *Appl. Phys. Lett.* **92**, 152902 (2008).
- <sup>18</sup>B. D. Cullity, *X-Ray Diffraction* (Addison-Wesley, Reading, MA, 1967).
- <sup>19</sup>L. Mu, P. H. Seow, S. N. Ang, and S. S. Feng, *Colloid Polym. Sci.* **283**, 58 (2004).
- <sup>20</sup>C. S. Tu, C. L. Tsai, J. S. Chen, and V. H. Schmidt, *Phys. Rev. B* **65**, 104113 (2002).
- <sup>21</sup>N. F. Mott and E. A. Davis, *Electronic Processes in Non-Crystalline Materials* (Clarendon, Oxford, 1979).
- <sup>22</sup>D. Liu, X. Yao, and L. E. Cross, *J. Appl. Phys.* **71**, 5115 (1992).
- <sup>23</sup>M. Kumar and K. L. Yadav, *J. Appl. Phys.* **101**, 054105 (2007).
- <sup>24</sup>T. Y. Chen, S. Y. Chu, R. C. Chang, C. K. Cheng, C. S. Hong, and H. H. Nien, *Sens. Actuators, A* **134**, 452 (2007).
- <sup>25</sup>G. Shirane, J. D. Axe, J. Harada, and J. P. Remeika, *Phys. Rev. B* **2**, 155 (1970).
- <sup>26</sup>L. Benguigui, *Solid State Commun.* **11**, 825 (1972).
- <sup>27</sup>R. F. Soohoo, *Theory and Application of Ferrites* (Prentice-Hall, Englewood Cliffs, NJ, 1960).
- <sup>28</sup>V. G. Bhide and M. S. Multani, *Phys. Rev.* **149**, 289 (1966).
- <sup>29</sup>M. K. Roy, B. Haldar, and H. C. Verma, *Nanotechnology* **17**, 232 (2006).